Full-Duplex Transmission Optimization for Bi-directional MIMO links with QoS Guarantees

Hiroki Iimori[†] and Giuseppe Abreu[‡]
[†] Dep. of EEE, Ritsumeikan University
1-1-1 Noji-higashi, Kusatsu, Shiga, 525-8577 Japan
[h.iimori,g.abreu]@gabreu.se.ritsumei.ac.jp
[‡] Dep. of CS. & EE., Jacobs University Bremen
Campus Ring 1, 28759, Bremen, Germany
g.abreu@jacobs-university.de

George C. Alexandropoulos
Mathematical and Algorithmic Sciences Lab
Huawei Technologies France SASU
92100 Boulogne-Billancourt, France
george.alexandropoulos@huawei.com

***Abstract*—We consider a bi-directional Full-Duplex (FD) Multiple-Input Multiple-Output (MIMO) communication system in which nodes are capable of performing transitter (TX)-Receiver (RX) digital precoding/combining and multi-tap analog cancellation, and have individual Signal-to-Interference-plus-noise Ratio (SINR) requirements. We present an iterative algorithm for the TX powers minimization that includes closed-form expressions for the TX/RX digital beamformers at each algorithmic iteration step. Our representative simulation results demonstrate that the proposed algorithm can reduce residual Self-Interference (SI) due to FD operation to below -110dB, which is the typical noise floor level for wireless communications. In addition, our design outperforms relevant recent solutions proposed for 2-user MIMO systems (the so called MIMO X channel) in terms of both power efficiency and computational complexity.**

***Index Terms*—Full-duplex MIMO, Beamforming (BF), self-interference cancellation, power minimization, optimization.**

I. Introduction

Motivated by the exponentially increasing demand for higher information rate under limited wireless resources, and propelled by recent advances in radio frequency (RF) hardware, in-band Full-Duplex (FD) radio has emerged as a key technology for future wireless applications from fifth generation (5G) mobile communication systems to Internet of Things (IoT) [1]–[3].

Practical communication in FD mode requires dedicated solutions to mitigate the Self-Interference (SI) caused by leakage of TX signals into the Receiver (RX) chain, due to the close proximity between transitter (TX) and RX antennas [4], [5]. Ironing out this fundamental issue of FD technology is one of the main research topics in this field, motivating various authors to contribute with several SI cancellation techniques for FD systems [1], [6]–[8].

Thanks to the added Degrees of Freedom (DoF) afforded by multiple antennas, bi-directional FD radio systems with high spectral efficiency can be designed exploiting MIMO technology [9]–[12]. In particular, hybrid MIMO SI suppressing techniques combining analog and digital cancellers have been proposed for FD radios [13]–[16] which proved very effective from a theoretical standpoint. From a practical implementation standpoint, however, it has been recently demonstrated in real-world experiments that such MIMO approaches are not devoid of its own technical challenges [1], [17], [18], one of which is the excessive cost incurred by the use of large numbers of antennas.

One approach to keep the hardware cost of hybrid MIMO SI suppressing techniques for FD radios under control is to reduce the number of antennas while introducing temporal DoFs by means of Tap Delay Line (TDL) processing in order to maintain the DoF required to achieve the desired performance [19]. In [19], for instance, a joint hybrid TX-RX BF design with limited hardware costs was proposed, in which the sum rate of a system with one MIMO FD radio communicating with two MIMO Half-Duplex (HD) nodes was optimized.

In this paper, we contribute to the area of effective and feasible SI canceller designs for MIMO FD radios as follows. First, we combine the joint hybrid TX-RX approach of [19] with the analog cancellation technique referred to as *multi-tap analog canceller* previously presented in [20]. The result is a new multi-tap *hybrid* (analog and digital) TX-RX MIMO FD SI cancellation scheme, in which the number of hardware components for analog cancellation becomes independent of the number of antennas. Secondly, instead of maximizing the sum rate (which is of less practical interest), we formulate our problem to minimize the TX power while guaranteeing (when possible) prescribed Quality of Service (QoS) targets defined in terms of maximum Signal-to-Interference-plus-noise Ratio (SINR). Thirdly and finally, we present a low-complexity solution to the latter problem in which the TX employs Maximum Ratio Transmission (MRT) with powers optimized in closed-form via a Perron-Frobenius (PF) method, while the RX maximizes the SINR by computing corresponding closed-form RX BF vectors from a Rayleigh Quotient (RQ), iteratively. Our results show that our algorithm can outperform the similar methods previously proposed for 2-user MIMO systems in terms of both power efficiency and computational complexity.

II. System Model

Consider the two-way FD MIMO communication system illustrated in Figure 1. This system consists of two node in which each equipped with M TX and N receive antennas. Both nodes are assumed to TX and receive simultaneously to/from one another in the same resource unit.

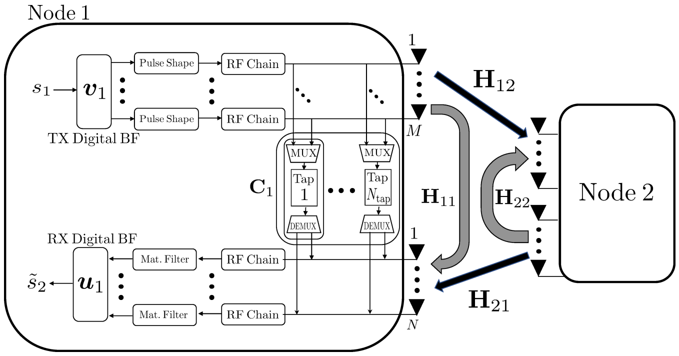

Fig. 1: System model of two-way full duplex MIMO with reduced hardware multi-tap analog cancellation.

A generic k-th node, with $k \in \{1,2\}$, is assumed to employ the digital TX precoding vector $\boldsymbol{v}_k \in \mathbb{C}^{M\times 1}$ and the digital RX BF vector $\boldsymbol{u}_k \in \mathbb{C}^{1\times N}$, as well as the multi-tap analog cancellation matrix $\boldsymbol{C}_k \in \mathbb{C}^{N\times M}$ [19], [20]. It is capable of performing TX-RX digital BF and analog SI cancellation with the aim at suppressing SI and maximizing rate simultaneously. Finally, in order to model practical limitations, it is assumed that the TXted signal at the k-th node has a power upper bound, such that $\mathrm{Tr}\left(\boldsymbol{v}_k\boldsymbol{v}_k^{\mathrm{H}}\right) = P_k \leq P_{\max}$.

Referring to Figure 1, let $\boldsymbol{H}_{k\ell} \in \mathbb{C}^{N\times M}$ and $\boldsymbol{H}_{kk} \in \mathbb{C}^{N\times M}$ be the intended channel matrix between the two nodes and the SI channel matrix at the k-th node, respectively, with $k \neq \ell \in \{1,2\}$. It is also assumed throughout this paper that each node has full knowledge of the Channel State Information (CSI) of both the communication links and their own SI link. Extension to imperfect CSI knowledge is left for future work.

From all the above, the received signal at the k-th node after applying analog SI cancellation can be written as

$$\begin{aligned} \boldsymbol{y}_k &= \boldsymbol{H}_{\ell k}\boldsymbol{v}_\ell s_\ell + \left(\boldsymbol{H}_{kk} - \boldsymbol{C}_k\right)\boldsymbol{v}_k s_k + \boldsymbol{n}_k \\ &= \underbrace{\boldsymbol{H}_{\ell k}\boldsymbol{v}_\ell s_\ell}_{\text{Intended}} + \underbrace{\tilde{\boldsymbol{H}}_{kk}\boldsymbol{v}_k s_k}_{\text{SI}} + \underbrace{\boldsymbol{n}_k}_{\text{Noise}}, \end{aligned} \tag{1}$$

where the multi-tap analog cancellation matrix $\boldsymbol{C}_k$ consists of N_{tap} non-zero components and $MN - N_{\text{tap}}$ zeros, $\boldsymbol{n}_k \sim \mathcal{CN}\left(0, \sigma^2 \boldsymbol{I}_N\right)$ denotes the complex Additive White Gaussian Noise (AWGN) vector under the assumption that $\boldsymbol{n}_k$ is independent from the TXted signal s_ℓ, and $\tilde{\boldsymbol{H}}_{kk} \triangleq \boldsymbol{H}_{kk} - \boldsymbol{C}_k$ is the SI channel matrix after performing the considered analog cancellation.

After digital down conversion and combining by the RX BF vector $\boldsymbol{u}_k$, the estimated signal $\tilde{s}_\ell$ corresponding to the intended signal s_ℓ at the k-th node can be expressed as

$$\begin{aligned} \tilde{s}_\ell &= \boldsymbol{u}_k \boldsymbol{y}_k \\ &= \boldsymbol{u}_k\boldsymbol{H}_{\ell k}\boldsymbol{v}_\ell s_\ell + \boldsymbol{u}_k\tilde{\boldsymbol{H}}_{kk}\boldsymbol{v}_k s_k + \boldsymbol{u}_k\boldsymbol{n}_k. \end{aligned} \tag{2}$$

Similarly, the received signal and symbol estimate at node $\ell \neq k$ after analog cancellation and RX BF are given, respectively, by

$$\boldsymbol{y}_\ell = \boldsymbol{H}_{k\ell}\boldsymbol{v}_k s_k + \tilde{\boldsymbol{H}}_{\ell\ell}\boldsymbol{v}_\ell s_\ell + \boldsymbol{n}_\ell, \tag{3}$$

$$\begin{aligned} \tilde{s}_k &= \boldsymbol{u}_\ell \boldsymbol{y}_\ell \\ &= \boldsymbol{u}_\ell\boldsymbol{H}_{k\ell}\boldsymbol{v}_k s_k + \boldsymbol{u}_\ell\tilde{\boldsymbol{H}}_{\ell\ell}\boldsymbol{v}_\ell s_\ell + \boldsymbol{u}_\ell\boldsymbol{n}_\ell, \end{aligned} \tag{4}$$

where $\boldsymbol{n}_\ell \sim \mathcal{CN}\left(0, \sigma^2\boldsymbol{I}_N\right)$ is the AWGN vector that is assumed independent from the TXted symbol s_k.

Assuming that unit power information signals s_k and s_ℓ are used, the average SINR estimates at the two nodes in Figure 1 can be, respectively, written as

$$\gamma_k = \frac{\left|\boldsymbol{u}_k\boldsymbol{H}_{\ell k}\boldsymbol{v}_\ell\right|^2}{\left|\boldsymbol{u}_k\tilde{\boldsymbol{H}}_{kk}\boldsymbol{v}_k\right|^2 + \sigma^2} \quad \text{and} \quad \gamma_\ell = \frac{\left|\boldsymbol{u}_\ell\boldsymbol{H}_{k\ell}\boldsymbol{v}_k\right|^2}{\left|\boldsymbol{u}_\ell\tilde{\boldsymbol{H}}_{\ell\ell}\boldsymbol{v}_\ell\right|^2 + \sigma^2}, \tag{5}$$

where we assume that the channel matrices in equation (5) are constant for a number of signal transmissions and the RX combining vector $\boldsymbol{u}_k, \forall k$ has a unit norm, i.e., $||\boldsymbol{u}_k||^2 = 1$.

III. QoS-Guaranteed Transmissions

Signal processing techniques for the joint TX-RX linear precoding/combining and adaptive TX power allocation with the aim of maximizing data rate while suppressing the residual SI power level have been proposed in the past [21], [22] demonstrating the feasibility of two-way FD MIMO systems.

Maximizing data rate is, however, not typically required by actual users, which instead tend to perceive the quality of a communication system by comparing it to a given level of expectation dictated by the intended application. We therefore consider instead the TX-RX beamformer optimization problem aiming at minimizing the individual TX powers while satisfying individual target SINR requirements:

$$\min_{\boldsymbol{v}_k, \boldsymbol{v}_\ell} \quad \sum_{k=1}^{2} ||\boldsymbol{v}_k||^2 \tag{6a}$$

$$\text{s.t.} \quad \gamma_k \geq \Gamma_k \ \ \forall k, \tag{6b}$$

where Γ_k is the target SINR for the k-th node.

A. TX Power Minimization with SINR Constraints

Let us define the normalized precoding vector $\bar{\boldsymbol{v}}_k \triangleq \frac{\boldsymbol{v}_k}{||\boldsymbol{v}_k||}$ and the TX power $P_k = ||\boldsymbol{v}_k||^2$ such that the optimization problem in (6) can be rewritten as

$$\min_{P_1, P_2} \quad \sum_{k=1}^{2} P_k \tag{7a}$$

$$\text{s.t.} \quad \gamma_k \geq \Gamma_k \ \ \forall k. \tag{7b}$$

The optimization problem described by equation (7) is well-known to be non convex due to the SINR constraints [23], although approximate solutions can be obtained for it with basis on convex optimization algorithms, such as interior point methods if the constraint can be convexified [24]. In addition to the losses due to convex relaxation, such solutions tend also to be computationally demanding. Therefore, we propose instead a low complexity alternating minimization method based on closed-form expressions of the optimal TX powers P_1 and P_2.

In order to obtain the desired closed-form expressions for P_1 and P_2, notice that from equation (5) and (7) we readily obtain

$$P_2\left|\boldsymbol{u}_1\boldsymbol{H}_{21}\bar{\boldsymbol{v}}_2\right|^2 \geq \Gamma_1\left(P_1\left|\boldsymbol{u}_1\tilde{\boldsymbol{H}}_{11}\bar{\boldsymbol{v}}_1\right|^2 + \sigma^2\right), \tag{8a}$$

$$P_1\left|\boldsymbol{u}_2\boldsymbol{H}_{12}\bar{\boldsymbol{v}}_1\right|^2 \geq \Gamma_2\left(P_2\left|\boldsymbol{u}_2\tilde{\boldsymbol{H}}_{22}\bar{\boldsymbol{v}}_2\right|^2 + \sigma^2\right). \tag{8b}$$

The latter inequalities can be re-expressed in matrix form a

$$\left(\mathbf{I}-\mathbf{\Gamma}\boldsymbol{M}\right)\boldsymbol{p}\geq\sigma^{2}\mathbf{\Gamma}\boldsymbol{m}, \qquad ($$

where we define the TX power vector $\boldsymbol{p}\triangleq[P_1,P_2]^{\mathrm{T}}$ and t auxiliary matrices $\mathbf{\Gamma}$, $\boldsymbol{M}$ and $\boldsymbol{m}$ respectively by

$$\mathbf{\Gamma} = \begin{bmatrix} 0 & \Gamma_2 \\ \Gamma_1 & 0 \end{bmatrix}, \qquad (10$$

$$\boldsymbol{M} = \begin{bmatrix} \frac{|\boldsymbol{u}_1\tilde{\boldsymbol{H}}_{11}\bar{\boldsymbol{v}}_1|^2}{|\boldsymbol{u}_1\boldsymbol{H}_{21}\bar{\boldsymbol{v}}_2|^2} & 0 \\ 0 & \frac{|\boldsymbol{u}_2\tilde{\boldsymbol{H}}_{22}\bar{\boldsymbol{v}}_2|^2}{|\boldsymbol{u}_2\boldsymbol{H}_{12}\bar{\boldsymbol{v}}_1|^2} \end{bmatrix}, \qquad (10$$

$$\boldsymbol{m} = \left[\left|\boldsymbol{u}_1\boldsymbol{H}_{21}\bar{\boldsymbol{v}}_2\right|^{-2} \quad \left|\boldsymbol{u}_2\boldsymbol{H}_{12}\bar{\boldsymbol{v}}_1\right|^{-2}\right]^{\mathrm{T}}. \qquad (10$$

Taking advantage of the PF theorem [25] and the fact th $\mathbf{\Gamma}\boldsymbol{M}$ is a non negative matrix, the optimal TX power vect can be computed in closed form as

$$\boldsymbol{p}^{*}=\sigma^{2}\left(\mathbf{I}-\mathbf{\Gamma}\boldsymbol{M}\right)^{-1}\mathbf{\Gamma}\boldsymbol{m}. \qquad (11)$$

B. Optimal BF Design for SINR Maximization

With possession of a closed-form optimal solution to the TX power vector $\boldsymbol{p}$ as per equation (11), as well as a given analog cancellation matrix $\boldsymbol{C}_k$ obtained for example as discussed in [19], [22], we seek optimal BF designs for $\boldsymbol{v}_k$ and $\boldsymbol{u}_k$ $\forall k$, such that the average SINR at each node is maximized, while minimizing the effect of the SI. Taking into account the fact that the role of TX-RX beamformers is to minimize the effect of SI while maximizing the downlink rate, we consider the MRT TX beamformer with perfect CSI known at the nodes, such that the instantaneous SINR at each node is maximized under the assumption that the SI power level can be significantly reduced after processing by the proposed optimal RX combiner.

1) Design of RX Combiner $\boldsymbol{u}_k\forall k$:

The role of the RX combining vector $\boldsymbol{u}_k$ at the k-th node is to maximize the power of the signal from the ℓ-th node, while supressing the interference-plus-noise signal. In other words, the RX BF vector $\boldsymbol{u}_k$ must be designed so as to maximize the ratio between the power of the intended signal and that of interference-plus-noise term of equation (2), which can be mathematically expressed as

$$\max_{\substack{\boldsymbol{u}_k \\ ||\boldsymbol{u}_k||^2=1}} \frac{\boldsymbol{u}_k \overbrace{\boldsymbol{H}_{\ell k}\boldsymbol{v}_{\ell}\boldsymbol{v}_{\ell}^{\mathrm{H}}\boldsymbol{H}_{\ell k}^{\mathrm{H}}}^{\triangleq\boldsymbol{Q}_{\boldsymbol{u}_k}}\boldsymbol{u}_k^{\mathrm{H}}}{\boldsymbol{u}_k \underbrace{\left(\tilde{\boldsymbol{H}}_{kk}\boldsymbol{v}_k\boldsymbol{v}_k^{\mathrm{H}}\tilde{\boldsymbol{H}}_{kk}^{\mathrm{H}}+\sigma^2\mathbf{I}\right)}_{\triangleq\boldsymbol{W}_{\boldsymbol{u}_k}}\boldsymbol{u}_k^{\mathrm{H}}}, \qquad (12)$$

which holds a generalized RQ structure, such that the optimal solution to $\boldsymbol{u}_k$ is obtained by [26]

$$\boldsymbol{u}_k^{*}=\mathrm{eigv}_{\max}\left(\boldsymbol{W}_{\boldsymbol{u}_k}^{-1}\boldsymbol{Q}_{\boldsymbol{u}_k}\right)^{\mathrm{H}}. \qquad (13)$$

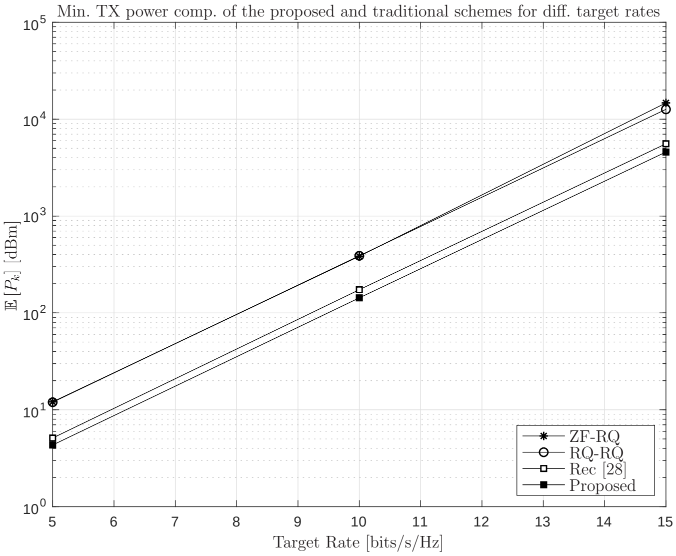

Fig. 2: Proposed and conventional preceding methods TX power comparison for different target rates.

Algorithm 1 Alt. TX Power Min. with SINR Guarantees.

1: **Input**:$P_k, \boldsymbol{H}_{kk}, \boldsymbol{H}_{\ell k},\ \boldsymbol{C}_k\forall k$ given by [19].
2: Set $P_k = P_{\max}\forall k\in\{1,2\}$ and make arbitrary unit-norm vectors as initial RX BF vectors $\boldsymbol{u}_k\forall k$.
3: **repeat**
4: Compute $\bar{\boldsymbol{v}}_k\forall k$ from equation (14).
5: Compute $\boldsymbol{u}_k^{*}\forall k$ from equation (13).
6: Compute $\boldsymbol{p}^{*}$ from equation (11).
7: **until convergence or reach maximum iterations.**

---

2) Design of TX Precoder $\boldsymbol{v}_k\forall k$:

Assuming that the strong SI caused by the leakage of own TX signals due to the close proximity of TX and RX antennas can be sufficiently suppressed by the RX combining vector $\boldsymbol{u}_k$, the role of the TX precoder $\boldsymbol{v}_k$ is only to direct the TX beams so as to maximize the downlink rate. For this purpose, it suffices to apply a simple MRT TX precoder, namely

$$\bar{\boldsymbol{v}}_k=\frac{\boldsymbol{H}_{kl}^{\mathrm{H}}\boldsymbol{u}_{\ell}^{\mathrm{H}}}{||\boldsymbol{H}_{kl}\boldsymbol{u}_{\ell}||}. \qquad (14)$$

Taking into account all the steps described in this section, the proposed algorithm for the optimization of TX powers, as well as TX and RX BF vectors can be compactly described by the pseudo-code offered in Algorithm 1.

IV. Simulation results

In this section, we evaluate the proposed iterative algorithm in terms of consumed TX power for different required SINR constraints via software simulation. The downlink communication channels $\boldsymbol{H}_{12}$ and $\boldsymbol{H}_{21}$ are assumed to be block Rayleigh fading with 110dB path loss, while the SI channels $\boldsymbol{H}_{11}, \boldsymbol{H}_{22}$ are assumed to be block Ricean with path loss of 40dB and K-factor 35dB [19], [27].

Each node is assumed to be equipped with 4 TX and receive antennas, i.e., $M=N=4$, with a noise floor of -110dBm, and the number of analog cancellation taps N_{tap} is set to 8, which corresponds to 50% reduction in the number of elements in the analog cancellation matrix $\boldsymbol{C}_k$ compared to [1], [6].

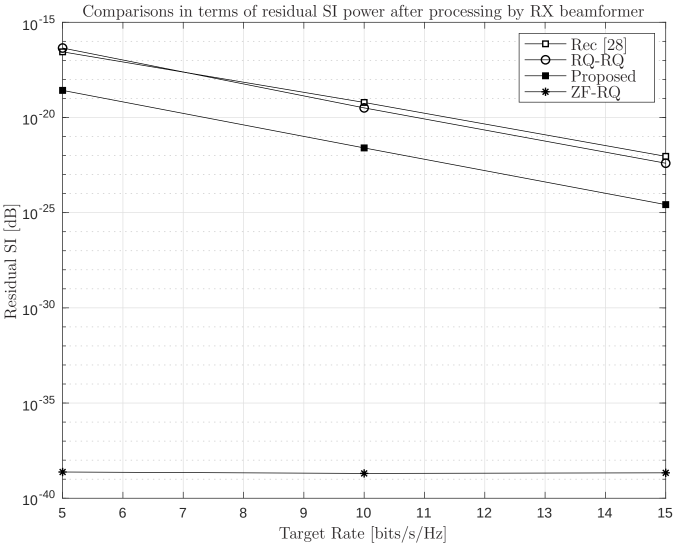

Fig. 3: Residual SI power comparisons of the proposed and conventional methods for different target rates after RX BF.

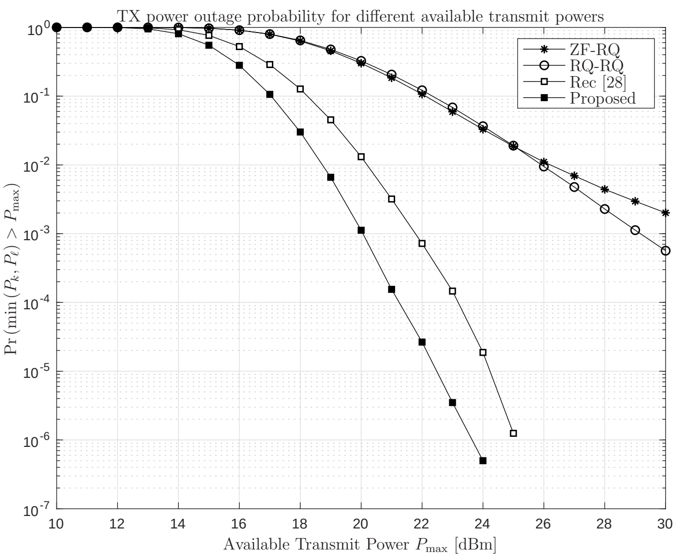

Fig. 4: TX power outage probability for different available TX powers with the fixed target rate $R_k = R_\ell = 8$ [bps/Hz].

For the modeling practical situations, the multi-tap analog canceller is assumed to be subjected to amplitude imperfection uniformly distributed between -0.01dB and 0.01dB and phase noise uniformly distributed between $-0.065°$ and $0.065°$ [19], [20].

In all figures that follow, we compare the proposed TX power minimization method in Algorithm 1 with 100 maximum iterations against the conventional Zero-Forcing (ZF) TX precoder, in which the proposed PF power optimization is applied. In addition, by noticing that the considered bi-directional FD MIMO corresponds to a special form of the MIMO X channel, we deploy relevant algorithms [28]–[30] targeting at TX-RX BF design yielding sum rate maximization. Particularly, our considered system is a MIMO X channel having $\boldsymbol{H}_{21}$ and $\boldsymbol{H}_{12}$ as the intended channels and $\tilde{\boldsymbol{H}}_{11}$ and $\tilde{\boldsymbol{H}}_{22}$ as the interference channels, having possibly larger powers than the intended ones.

TABLE I: Run time comparisons for different methods.

Methods	ZF	RQ-RQ	Rec	Proposed
Average run time [s]	0.0025	0.0028	0.1309	0.0022

First, average TX power comparisons of the proposed algorithm for different target rates $\log_2(1+\Gamma_k)\forall k$ is shown in Figure 2, where ZF-RQ, RQ-RQ [30] and the Reconfigurable sum rate maximization algorithm [28] are employed as a benchmark. In order to fairly compare those algorithms, we adopt an alternating recalculation between TX-RX BF for each algorithms until convergence or maximum number of iterations reached. It is shown in Figure 2 that the proposed method can decrease the TX power by about -4.5dB compared to the conventional ZF-RQ, RQ-RQ methods and about -0.8dB compared against the Reconfigurable method.

Secondly, Figure 3 outlines that the interference cancellation performance in terms of residual SI power levels after processing by the RX BF are compared for the different TX-RX BF schemes. From Figure 2 and 3, one can notice that although the ZF method can perfectly suppress the effect of SI at the RX baseband, the proposed method can outperform the other schemes due to the fact that not only the residual SI level of the proposed method is suppressed below the noise floor level but also it aims at maximizing the data rate performance. In other words, the other methods devote too much available DoFs to suppressing SI power level at the RX baseband.

Thirdly, the TX power outage probability of the proposed method for different available TX powers $P_{\max}$ with target data rate fixed at $R_k = R_\ell = 8$ [bps/Hz] is compared with the outage performance of the other conventional methods in Figure 4, where we define the TX power outage probability as $\Pr(\min(P_k, P_\ell) > P_{\max})$. Lastly, the average run time comparisons until the convergence for each different algorithms are depicted in TABLE I, where we take an average from 500 channel realizations. From Figure 2, 3 and 4 and Table I, it can be observed that the proposed method can has much fast convergence rate compared with the Reconfigurable method and outperform the conventional ZF and RQ TX BF methods in terms of the TX power outage probability performance.

V. Conclusion

In this paper, we considered bi-directional FD MIMO communications systems with limited number of analog canceller taps and designed TX-RX BF vectors with the goal to minimize TX power under SINR constraints.

The proposed TX power minimization BF design was investigated in terms of system performance and complexity, and the PF TX power minimization approach was jointly offered with the proposed beamformers. Simulation results demonstrate the capability of our proposed algorithm to suppress the SI level to below -110dB which is the typical noise floor for wireless communications, while maximizing the downlink rate, and consequently, it minimizes the average TX power for different target data rate.

VI. Acknowledgement

Parts of this work were supported by JSPS KAKENHI, Grant Number JP17K06448, Denkitsushin Hukyu Foundation, and EU Project HIGHTS with grant number 636537.

References

[1] D. Bharadia, E. McMilin, and S. Katti, "Full duplex radios," in *Proc. ACM SIGCOMM.*, New York, NY, USA, 2013, pp. 375–386.

[2] D. Kim, H. Lee, and D. Hong, "A survey of in-band full-duplex transmission: From the perspective of PHY and MAC layers," *IEEE Commun. Surv. Tuts.*, vol. 17, no. 4, pp. 2017–2046, Feb. 2015.

[3] A. Sabharwal, P. Schniter, D. Guo, D. W. Bliss, S. Rangarajan, and R. Wichman, "In-band full-duplex wireless: Challenges and opportunities," *IEEE J. Sel. Areas Commun.*, vol. 32, no. 9, pp. 1637–1652, June 2014.

[4] Z. Zhang, X. Chai, K. Long, A. V. Vasilakos, and L. Hanzo, "Full duplex techniques for 5G networks: Self-interference cancellation, protocol design, and relay selection," *IEEE Commun. Mag.*, vol. 53, no. 5, pp. 128–137, May 2015.

[5] J. I. Choi, M. Jain, K. Srinivasan, P. Levis, and S. Katti, "Achieving single channel, full duplex wireless communication," in *Proc. MOBICOM*, New York, NY, USA, Sep. 20 - 24 2010, pp. 1–12.

[6] E. Everett, M. Duarte, C. Dick, and A. Sabharwal, "Empowering full-duplex wireless communication by exploiting directional diversity," in *Proc. Asilomar CSSC*, Nov. 2011, pp. 2002–2006.

[7] Y. Wang, Q. Jiang, Z. Chen, and B. Xia, "Outage probability of two-way full-duplex amplify-forward relay systems with asymmetric traffic requirements," in *Proc. IEEE WCSP*, Nanjing, China, 15-17 Oct. 2015, pp. 1–5.

[8] A. Altieri, L. R. Vega, P. Piantanida, and C. G. Galarza, "On the outage probability of the full-duplex interference-limited relay channel," *IEEE J. Sel. Areas Commun.*, vol. 32, no. 9, pp. 1–13, Sep. 2014.

[9] M. Vehkaperä, T. Riihonen, and R. Wichman, "Asymptotic analysis of full-duplex bidirectional MIMO link with transmitter noise," in *Proc. IEEE PIMRC*, London, UK, Sep. 2013, pp. 1265–1270.

[10] B. Day, A. Margetts, D. Bliss, and P. Schniter, "Full-duplex bidirectional MIMO: Achievable rates under limited dynamic range," *IEEE Trans. Signal Process.*, vol. 60, no. 7, pp. 3702–3713, Jul. 2012.

[11] S. Jia and B. Aazhang, "Signaling design of two-way MIMO full-duplex channel: Optimality under imperfect transmit front-end chain," *IEEE Trans. Wireless Commun.*, vol. 16, no. 3, pp. 1619–1632, March 2017.

[12] T. Riihonen, M. Vehkaperä, and R. Wichman, "Large-system analysis of rate regions in bidirectional full-duplex MIMO link: Suppression versus cancellation," in *Proc. IEEE CISS*, Baltimore, USA, Mar. 2013, pp. 1–6.

[13] N. M. Gowda and A. Sabharwal, "Jointnull: Combining reconfigurable analog cancellation with transmit beamforming for large-antenna full-duplex wireless," *IEEE Trans. Wireless Commun.*, vol. 17, no. 3, pp. 2094–2108, Mar. 2018.

[14] D. Korpi, L. Anttila, and M. Valkama, "Reference receiver based digital self-interference cancellation in mimo full-duplex transceivers," in *Proc. IEEE GLOBECOM*, Austin, USA, Dec. 2014.

[15] M. S. Sim, M. Chung, D. Kim, J. Chung, D. K. Kim, and C.-B. Chae, "Nonlinear self-interference cancellation for full-duplex radios: From link-level and system-level performance perspectives," *IEEE Commun. Mag.*, vol. 55, no. 9, Jun. 2017.

[16] A. C. Cirik, R. Wang, and Y. Hua, "Weighted-sum-rate maximization for bi-directional full-duplex MIMO systems," in *Proc. Asilomar CSSC*, Nov. 2013.

[17] M. Jain, J. I. Choi, T. M. Kim, D. Bharadia, S. Seth, K. Srinivasan, P. Levis, S. Katti, and P. Sinha, "Practical, real-time, full duplex wireless," in *Proc. ICMCN*, New York, USA, Sep. 2011, pp. 301–312.

[18] D. Korpi, J. Tamminen, M. Turunen, T. Huusari, Y. S. Choi, L. Anttila, S. Talwar, and M. Valkama, "Full-duplex mobile device: Pushing the limits," *IEEE Commun. Mag.*, vol. 54, no. 9, pp. 80–87, Sep. 2016.

[19] G. C. Alexandropoulos and M. Duarte, "Joint design of multi-tap analog cancellation and digital beamforming for reduced complexity full duplex MIMO systems," in *Proc. IEEE ICC*, Paris, France, 21–25 May 2017, pp. 1–7.

[20] K. E. Kolodziej, J. G. McMichael, and B. T. Perry, "Multitap RF canceller for in-band full-duplex wireless communications," *IEEE Trans. Wireless Commun.*, vol. 15, no. 6, pp. 4321–4334, Jun. 2016.

[21] G. Zheng, "Joint beamforming optimization and power control for full-duplex MIMO two-way relay channel," *IEEE Trans. Signal Process.*, vol. 63, no. 3, pp. 555–566, Feb. 2015.

[22] H. Iimori and G. Abreu, "Two-way full-duplex MIMO with hybrid TX-RX MSE minimization and interference cancellation," in *Proc. IEEE SPAWC*, Kalamata, Greece, Jun. 2018, pp. 1–6.

[23] S. Malla and G. Abreu, "Transmission strategies under imperfect instantaneous CSIT," in *Proc. IEEE WCNC*, New Orleans, USA, Mar. 2015, pp. 1–6.

[24] S. P. Boyd and L. Vandenberghe, *Convex Optimization*. Cambridge University Press, 2004.

[25] S. U. Pillai, T. Suel, and S. Cha, "The Perron-Frobenius theorem–Some of its applications," *IEEE Signal Processing Mag.*, vol. 22, no. 2, pp. 62–75, March 2005.

[26] R. Prieto, "A general solution to the maximization of the multidimensional generalized Rayleigh quotient used in linear discriminant analysis for signal classification," in *Proc. IEEE ICASSP*, vol. 6, Hong Kong, China, Apr. 2003, pp. 1–4.

[27] M. Duarte, C. Dick, and A. Sabharwal, "Experiment-driven characterization of full-duplex wireless systems," *IEEE Trans. Wireless Commun.*, vol. 11, no. 12, pp. 4296–4307, Dec. 2012.

[28] G. C. Alexandropoulos and C. B. Papadias, "A reconfigurable iterative algorithm for the K-user MIMO interference channel," *Signal Process.*, vol. 93, no. 12, pp. 3353–3362, Jun. 2013.

[29] G. C. Alexandropoulos, P. Ferrand, J.-M. Gorce, and C. B. Papadias, "Advanced coordinated beamforming for the downlink of future LTE cellular networks," *IEEE Commun. Mag.*, vol. 54, no. 7, pp. 54–60, Jul. 2016.

[30] O. Taghizadeh, A. C. Cirik, and R. Mathar, "Hardware impairments aware transceiver design for full-duplex amplify-and-forward MIMO relaying," *IEEE Trans. Wireless Commun.*, vol. 17, no. 3, pp. 1644–1659, Dec. 2018.